Chapter 3
Positron Emission Tomography (PET) Use in Pharmacology

Jonathon A. Nye and Leonard Howell

Abstract Positron emission tomography (PET) is a sensitive and specific noninvasive imaging technology used to measure the 3-dimensional distribution of molecules and their functional outcome over time. This is achieved by detecting the annihilation photons resulting from the decay of radioisotopes (i.e., oxygen-15, nitrogen-13, carbon-11, fluorine-18) chemically labeled to biologically active molecules. The functional fate of these radiolabeled molecules may be determined by examining the images formed from the 3-dimensional reconstruction of the decay events. The approximate sensitivity of PET is picomolar, which permits the injection of molecular masses far below that known to disturb most physiological processes. This methodology is known as the "tracer technique" and is the basic analysis principle used to extract quantitative information from PET images. PET has the ability to provide valuable information related to functional processes of the body including blood flow, transport rates, receptor density, and drug occupancy. This chapter focuses on the physics of PET and its use in answering questions related to pharmacology. The basic principles of PET imaging will be reviewed followed by methods to derive quantitative information related to physiology from the image data. The application of compartmental modeling will be discussed in detail as will potential pitfalls that can occur during data collection.

Keywords Positron emission tomography (PET) • Tracer technique • Compartmental modeling • Dosimetry • Radioisotopes

J.A. Nye, PhD (✉)
Department of Radiology and Imaging Services, Emory University School of Medicine, 1841 Clifton Road NE, Room 205, Atlanta, GA 30329, USA
e-mail: jnye@emory.edu

L. Howell, PhD
Division of Neuropharmacology and Neurologic Diseases, Yerkes National Primate Research Center, Emory University, Atlanta, GA USA
e-mail: lhowell@emory.edu

M. Jann et al. (eds.), *Applied Clinical Pharmacokinetics and Pharmacodynamics of Psychopharmacological Agents*,
DOI 10.1007/978-3-319-27883-4_3

Positron emission tomography (PET) is a sensitive and specific noninvasive imaging technology used to measure the 3-dimensional distribution of molecules and their functional outcome over time. This is achieved by detecting the annihilation photons resulting from the decay of radioisotopes (i.e., oxygen-15, nitrogen-13, carbon-11, fluorine-18) labeled to biologically active molecules. The functional fate of these radiolabeled molecules may be determined by examining the images formed from the 3-dimensional reconstruction of the decay events. The approximate sensitivity of PET is picomolar, which permits the injection of molecular masses far below that known to disturb most physiological processes. This methodology is known as the "tracer technique" and is the basic analysis principle used to extract quantitative information from PET images.

The design of the biochemically active molecule depends on the system to be studied and may be endogenous or an analogue to the functional system. As an example, the most widely used radiotracer in PET is fluorine-18 labeled glucose ([F-18]FDG). In the synthesis of this compound, a hydroxyl group is replaced with an F-18 atom resulting in a nonnatural analogue of glucose. The analogue nature of [F-18]FDG is advantageous as the radiotracer completes only a few metabolic steps compared to glucose and eventually becomes trapped within a cell following phosphorylation. The in vivo fate of [F-18]FDG can be modeled by assigning compartments to processes that lead to the trapping of [F-18]FDG [1]. The rate constants describing the movement of [F-18]FDG between these compartments are solved for using principles of pharmacology, which allow for the estimation of regional glucose metabolism. PET has the ability to provide valuable information related to functional processes of the body including blood flow, transport rates, receptor density, and drug occupancy.

This chapter focuses on the physics of PET and its use in answering questions related to pharmacology. The basic physical principles of PET imaging will be reviewed followed by methods to derive quantitative information related to physiology from the image data. The application of compartmental modeling will be discussed in detail as will potential pitfalls that can occur during data collection.

3.1 Physical Principles of PET Imaging

PET takes advantage of the unique characteristics of positron decay. The purpose of the decay is to shed positive charge and reach a stable energy state. This decay process results in a daughter isotope with an atomic number one less than the parent. For example, the positron decay of fluorine-18 results in stable oxygen-18. Upon decay of the positron, the particle will expend its kinetic energy through scatter and ionization events up to a distance of approximately 1–2 mm from the decay origin. Once the positron has expended its kinetic energy, it meets its antiparticle, an electron and annihilates. The annihilation results in two nearly colinear 511 keV photons. Detection of these photons is accomplished by a ring of detectors; therefore, a pair of annihilation photons is ideally detected by opposing detectors which

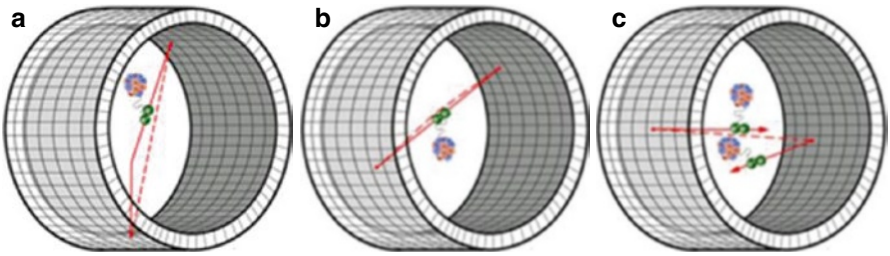

Fig. 3.1 Three types of events recorded by a 3D PET scanner are shown. The annihilation event occurs several millimeters from the decay origin. The *dotted line* represents the line of response, along which the scanner assigns the decay event. (**a**) Scatter event, one annihilation photon undergoes Compton scattering before reaching the detector. (**b**) True event, both annihilation photons reach opposing detectors uninhibited. (**c**) Random event, two unrelated annihilation photons from separate decay events reach the detectors

is called coincidence detection. The two opposing detectors form a line in space, called a line of response (LOR), along which it is highly probable the original decay event occurred. If a sufficient number of these events are recorded, the information can be used to estimate the location of radioactive sources in a 3-dimensional volume. This process is called tomography, where 2D projections are collected over many angles and used to recreate the 3-dimensional distribution of the radioactive sources.

For a subject injected with a radiotracer that emits positrons, the resulting annihilation photons are detected by a cylindrical ring of scintillation crystals. Scanners are made of several rings sandwiched together, and all detectors are continuously monitoring for photons. The number of photons intercepting these detectors will depend on the mode of operation. In 2-dimensional mode, annihilation photons detected are restricted to a single detector ring by lead collimation placed between each ring. In 3-dimensional mode, the lead collimation is absent and annihilation events are free to cross between rings, substantially increasing sensitivity of detection but also presenting additional challenges (Fig. 3.1).

The process of detection is not perfect and is statistically bound by the conversion of light to electrical signal; thus, a PET scanner will accept a range of photon energies (450–600 keV). The photons detected in the scintillation crystals are converted to an electrical signal, and from that signal, the photon energy, location, and time of its arrival at the detector are recorded. Knowing the time is critical. If two opposing detectors recorded an event within a very short coincidence timing window (i.e., a few nanoseconds), then there is a high probability that the photons originated from a single annihilation event. These events are assigned to an LOR and called prompt coincidence events.

In recording the energy of the detection event, it is important to know whether the annihilation photon interacted with tissue in the body prior to its detection. If the recorded energy is 511 keV, then it is overwhelmingly likely the photon did not interact with tissue in its flight to the detector. Events with less energy suggest the

photon lost energy by scattering in the body and that its current line of trajectory does not include the origin of the annihilation event.

There are four categories of prompt coincidence events: true, random, scatter, and multiple. True events (Fig. 3.1b) occur when both photons originate from a single annihilation source and intercept the detectors at their original energy, 511 keV. These events occur within the coincidence timing window and are the most desirable. The reconstruction of these events will estimate the distribution of the radioactive sources in the imaged volume. Random events (Fig. 3.1c) may also occur in the coincidence timing window; however, their occurrence results from two 511 keV photons that originated from separate annihilation events. The resulting LOR does not accurately represent the location of an annihilation event. These events are random in time and space and add a uniform background to the image. Fortunately, the randomness in time can be exploited by choosing a coincidence window of which true events cannot occur; thus, the random rate can be measured directly during the data acquisition process.

A scatter event (Fig. 3.1a) is when one of the annihilation photons interacts with tissue resulting in a transfer of energy to the tissue and a change in trajectory from its original path. The greater the angle of scatter from its original trajectory, the greater the amount of energy transferred to the tissue. If enough energy is lost in the scatter event, that photon's energy will fall below the accepted photon energy range of the scintillation detectors and the event will not be recorded. If a scattered photon is recorded, then it will be assigned an LOR. Again, this LOR will not include the origin of the original annihilation event. The recording of scatter events increases the background causing a loss of image contrast. These events cannot be measured during the data collection and therefore are modeled using specialized software. The last event type is a multiple event, which is a combination of a true and random event resulting in three detected events within the coincidence window. These combinations of events result in three possible LORs, but it is unknown which is the true LOR. Typically one can be eliminated because one of the LORs is outside the field of view. What is left over is a random and true LOR. Correction of the randoms should reveal the true LOR. Overall, these events are rare.

There is one event that is not recorded in the prompt dataset: an attenuation event. Attenuation is the loss of annihilation events because they are either absorbed in the tissue or scattered outside the detector plane. Attenuation depends on the total path length traveled by the annihilation photons. Therefore, photons originating from the center of an object have a greater probability of being attenuated compared to those originating from the periphery of the object. The result of attenuation is a depressed signal in center of the image compared to the periphery. Estimating these lost events is relatively straightforward and can be accomplished by collecting transmission data of the object as explained in the next section.

The spatial resolution of PET is limited by a few primary physical factors: detector size, positron range, and non-colinearity of the annihilation photons. Discrete detectors are used to monitor photons which are constructed as long rectangular columns focused at the center of the scanner. Their size range from

4–8 mm on the face and 20–30 mm in depth. The limiting resolution of a detector is approximately half the size on the face, or about 3–4 mm. Secondly, during a decay event, the positrons carry kinetic energy and travel a finite distance expending that energy into surrounding tissue before annihilating with an electron. The higher the kinetic energy of the positron, the greater the distance traveled from its decay origin. This distance adds uncertainty to the location of the original decay site and contributes to resolution degradation in the reconstructed image. Lastly the majority of annihilation events do not result in perfectly colinear 511 keV photons because some residual momentum is left with the positron at the time of annihilation. The loss in spatial resolution of non-colinear photons is ~0.2 % of the detector ring diameter, which for an 80 cm ring can be as high as 2 mm. These three physical factors of the detection process limit the intrinsic resolution of a PET scanner to approximately 6 mm in an 80 cm detector ring. Constructing a scanner with smaller detectors and a smaller ring diameter will improve the intrinsic resolution, but as the size decreases, the positron range will eventually dominate the resolution degradation.

Objects smaller than the spatial resolution of the PET system can still be resolved in an image, but the measured radioactivity concentration and contrast are diminished compared to the truth. The spatial resolution of a system is measure by placing a point object in the scanner field of view and collecting an image. The resulting image is a sphere with an intensity profile that is Gaussian, having a full width of 3–4 mm at half maximum (FWHM). This is called the system's point spread function. A PET system is able to correctly measure the true radioactivity concentration when the measured object is greater than twice the resolving volume (2 × FWHM) of the system. When imaging volumes are smaller than the resolving volume of the PET systems, the pixel intensities in the reconstructed image no longer represent the true concentration. This physical effect is called the partial volume problem. However, this loss in signal can be modeled and corrected using methods of partial volume correction.

3.2 Corrections and Image Formation

The basic approach to image formation is the process of using 2D projections to estimate the 3D distribution of radioactivity in a structure. This can be done using stacks of 2D or fully 3D projection data. The image formation process is called reconstruction, and two general methods are available: (1) a direct inversion process called filtered back projection (FBP) and (2) an iterative process called maximum likelihood expectation maximization. The former algorithm requires fewer computational recourses compared to expectation maximization but is limited by assumptions that include geometric invariance across the field of view, noiseless data, perfect corrections for true events, and no gaps in the tomographic projections. These assumptions are not necessary for expectation maximization because the physics of the photon interactions and scanner geometry among other aspects can

be included in the algorithm during reconstruction. However, before the projection data can be reconstructed into an image, corrections need to be made to address random events, scatter events, and attenuation effects in the prompt dataset.

As briefly discussed above, random events are random in time and space. These events are measured in two ways: (1) direct measurement using a delayed window or (2) estimated from the single 511 keV count rates between opposing detectors. The estimate of randoms is obtained for all LORs and subtracted from the prompt dataset resulting in the sum of the true and scatter coincidence events. Ideally, a randoms fraction <10 % of the prompt rate is considered desirable, as this rate will not overly tax the counting electronics. Scatter in a dataset leads to a reduction in contrast and resolution. The distribution of scatter in an image is dependent on the structure of the object, and the probability of scatter is higher for LORs that pass through the center of an object. Thus, a reconstructed image without scatter correction will have the appearance of higher radioactivity at the center of the object. Scatter correction is a difficult problem because the source of a scattering event depends on the radioactivity distribution and attenuating structures of the object. PET instruments are not sensitive enough to measure scatter directly; thus, scatter is estimated using knowledge of the radioactive and structural source distributions. The algorithms that are most commonly used are the single scatter simulation, convolution scatter correction methods, and a Gaussian fitting technique. Two fundamental difficulties can result in the application of these algorithms. First, these methods operate on measured data collected inside the field of view; thus, sources of radioactivity outside the field of view are unknown. Scatter from outside the field of view is typically overcome by calculating the shape of the scatter profile and then scaling to scattered radioactivity measured outside the object. The second difficulty is estimating scatter at low count rates where scaling of the profile can be erroneous due to increased uncertainty in the detected scatter events. The total scatter in the prompt dataset depends on the mode of operation. The scatter signal comprises approximately 10–15 % of the prompt dataset in 2D imaging and 40–50 % of the prompt dataset in 3D imaging. Scatter correction is performed by subtracting the estimated scatter from the prompt dataset resulting in the sum of true coincidence events.

Attenuation correction estimates the loss of signal in a dataset due to photons absorbed in the object or scattered outside the field of view. For a 20 cm diameter object, this signal loss can be as high as a factor of ×7 in the center of the object. For PET, attenuation of an object depends on the total path length traveled along an LOR. The total attenuation can be measured directly by placing a source of radioactivity at the edge of the field of view and acquiring counts with and without the object in the scanner. The logarithm of the ratio of these measurements will give the attenuation factor for a given line of response. Traditionally, the transmission scan is accomplished using an external sealed radioactive source (Ge-68, Cs-137, Co-57) that is rotated around the object for several minutes. In modern clinical PET systems, the transmission scan is acquired using a computed tomography (CT) scanner. These hybrid (PET/CT) systems provide two major advantages compared to traditional systems. First, the CT provides anatomical detail that can be fused with the

PET reconstruction for localization and correlation of radiotracer uptake with anatomy. Second, CT imaging is a high photon statistical process that provides nearly noiseless data when compared to external rotating sources, thereby minimizing the propagation of transmission data noise into the reconstructed image. Attenuation correction is performed by multiplying the true coincidence events by a set of attenuation correction factors.

When randoms, scatter, and attenuation corrections have been made to the data, the final result should be a dataset made up of true events. FBP requires that the corrections to randoms, attenuation, and scatter be performed perfectly prior to reconstruction. There are additional corrections needed to meet the requirements for filtered back projection, including scanner geometry and detector efficiency. Although great effort is spent in instrument calibration and computational resources to generate these corrections, invariably a breakdown does occur in the FBP assumptions, and the results can be observed in the image. Poisson noise in the individual lines of response results in streaks in the images radiating out from the center of the field of view. This is most apparent outside the object where both positive and negative streaks occur. Some level of image artifacts due to the FBP process should be acceptable to take advantage of the fast reconstructions offered by this algorithm.

The iterative reconstruction process is not constrained by the same assumptions as FBP but does have drawbacks. The process of iterative reconstruction can incorporate many aspects of the imaging process into the algorithm to compute the most likely source distribution that created the prompt dataset. The iterative process begins with a guess of the source distribution. The scanning process is then simulated by forward projecting the guess to create a simulated prompt dataset. The simulated dataset is then compared to the measured prompt dataset, and a correction for the guess image is created. The guess image is then updated, and the process occurs repeatedly through several iterations until the simulated data match, or closely match, the measured dataset. The advantage of the iterative reconstruction process is the inclusion of the corrections (i.e., randoms, scatter, and attenuation). Poisson count statistics and other physical scan processes are factored into the scanning simulation step of the algorithm. The result is an image that is much more accurate, as noted by a visual improvement in contrast and noise compared to FBP. The drawback of the iterative method is a substantial increase in computational time. The process of simulating the scanner physics is time consuming, and increasing the number of corrections adds to the computing time. A second drawback is deciding how many iterations are necessary for the simulated data to be considered matched to the measured dataset. Because the decay and acquisition process follow well-known Poisson distributions, the decision can be made by probabilistically comparing the datasets. In general, there are a number of iterations that when exceeded result in an incremental improvement in the guess image; thus, a fixed number of iterations is chosen for practical reasons. The choice of using FBP or iterative reconstruction is often a legacy matter, but as computation power increases, iterative reconstruction has become preferred.

3.3 Quantification

PET offers the possibility of absolute quantitative measurements of radiotracer concentration in vivo. This implies that the voxel intensities are directly proportional to the radioactivity concentration. There are several methods of image processing to extract physiologically relevant data from PET images, from the simplistic data normalizations to mathematical modeling of radiotracer time-courses. Whatever the needed information from the analysis of image data, it is desirable that the process be easily reproducible and reliable across subjects with various biological states. This would permit studying populations or the progression/inhibition of biological states in an individual before and after treatment. The purpose of this section is to describe techniques to quantify PET image data.

3.3.1 Standardized Uptake Value

The standardized updake value (SUV) is a dimensionless quantity (g/mL) that is calculated by normalizing the measured radiotracer concentration in a target tissue to the ratio of the administered radioactivity and subject mass. This normalizing step is an attempt to compensate for the inter- and intra-subject variation and offers a fast and easy method of comparing radiotracer uptake in a target. The SUV is a function of time as the compound distributes and concentrates in tissues. Generally, given enough time post injection, the radiotracer will reach peak uptake or transient equilibrium. It is at one of these time points that SUV is typically evaluated. For a radiotracer evenly distributed throughout the body, the SUV would equate to one everywhere. An SUV value greater than one suggests that a physiological mechanism is actively involved in the concentration of a radiotracer. But SUVs are subject to variability from a number of sources such as the duration of the scan, physical decay correction, biological variations or nonsteady-state processes, inaccuracies in body weight (i.e., presence of fat), image noise, and scanner cross-calibration.

3.3.2 Target to Reference Tissue Ratios

The ratio of target-to-reference tissue regions improves the robustness of the quantification because it does not require calibration of the scanner. Secondly, the PET data do not need to be corrected for physical decay of the labeled radioisotope. The target tissue contains the molecular target, whether a transporter process, receptor site, or other cellular process. The reference tissue is a region that does not include the molecular target or has a negligible concentration. For example, the target tissue may be a region in the brain that expresses a receptor that exhibits specific binding for the radiotracer, but this receptor is absent in the reference region. Some

challenges are present with this method, as a tissue or region exhibiting negligible specific binding may not be available. Secondly, the target-to-reference tissue ratios are a function of time; therefore, care must be taken in selecting the most appropriate time point.

3.3.3 Kinetic Analysis

Quantitative image data from PET allows relationships to be inferred that relate the kinetics and distribution of a radiotracer to one or more physiological processes in the body. This usually requires dynamic imaging (acquiring multiple images of the radiotracer distribution over time) to observe the movement of radiotracer from region to region or its change within a region over time. Physiological information regarding processes responsible for the radiotracer's dynamic distribution can then be estimated with the help of a mathematical model. This concept has been used to determine a number of physiologically meaningful parameters such as blood flow, cellular metabolism, and receptor density. The mathematical model may be carried out using several approaches such as compartment modeling, graphical transformation, and evaluating the system at equilibrium.

The process of collecting dynamic PET data starts at the time of injection and extends for a duration long enough to capture the biochemical process of interest. The interval of successive images, or frames, should be on the order of the temporal changes of the radiotracer distribution. At the time of injection, the radiotracer enters the bloodstream through a peripheral vein and is quickly pumped though the pulmonary vasculature and the rest of the body. Early images of the radiotracer contain information primarily influenced by blood flow and interstitial tissue exchange and must be collected rapidly because the distribution changes quickly. Each successive pass of the radiotracer through the system is characterized by radiotracer leaving the blood and concentrating in the peripheral tissue for one reason or another. Over time the accumulated radioactivity is sensitive to differences in cell physiology. Therefore, a dynamic PET acquisition begins with short time frames to capture blood flow-dependent changes followed by gradually lengthening time frames to capture slower processes occurring within the tissues.

It is desirable to image for as long as the relative radiotracer distribution continues to change. However, the total imaging time is limited by physical, physiological, and practical considerations. First, the physical half-life of the labeling isotope limits the useful imaging time to approximately 3–4 half-lives. After more than about 4 half-lives, the reduced number of collected counts increases image noise, decreases image contrast, and leads to a less accurate estimate of the amount of radiotracer in tissue. Physiological factors such as organs that metabolize, concentrate, and excrete the radiotracer can confound image interpretation in areas surrounding those tissues. Lastly, practical limitations such as use of scanner time and patient or subject comfort will impose limits on the duration of an imaging study.

Considering these limitations, it is reasonable to assume that no matter the biochemical process of interest, approximately 2 h of useful imaging time (including positioning and transmission scanning) is available to collect information.

3.3.3.1 Compartment Modeling to Described PET Data

The reconstructed radioactivity concentration contained within a region or voxel in the PET image arrives from a combination of multiple signals including that from arterial blood and tissue. The influence of one signal versus the other depends on a variety of physiological mechanisms including transport from the plasma to the interstitial tissues and changes in the molecular state such as metabolism or binding to receptors. Each of these physiological spaces or states is assigned to a compartment. Each of these compartments varies over time in the region or voxel and can be described by a series of coupled first-order differential equations. The coefficients, representing the rate of radiotracer exchange between compartments, are assumed to be invariant over the duration of the study. The rate of exchange of radiotracer between compartments could be very interesting physiologically. For example, it could represent a metabolic rate, the rate that the radiotracer binds to a specific site which in turn is proportional to the number of binding sites, or the rate at which a radiotracer crosses a capillary membrane, which is in turn proportional to the amount of blood flowing into that capillary or tissue. The goal of modeling is to choose an appropriate number of compartments and their associated rate constants to permit the elucidation of pharmacokinetic parameter values that are of physiological importance.

The sophistication of the compartment model in PET imaging is limited due to spatial and temporal sampling as well as noise in the image. Image noise is the largest confounding factor and is influenced by a large number of variables in the processing of PET data, including camera sensitivity, radiotracer uptake, scan duration, reconstruction parameters and image corrections, and the size of the region of interest. One, two, or three compartments are generally sufficient to describe PET data. A series of compartments might consist of (1) free radiotracer in blood plasma, (2) free radiotracer in extracellular space, and (3) radiotracer in intracellular space. The free radiotracer in plasma is generally considered the first compartment and is measured from arterial blood (see Sect. 3.3.3.2). The compartments representing the extracellular and intracellular space are commonly referred to as “tissue” compartments; therefore, the above example is also termed a two-tissue compartment model where the plasma compartment is inferred. The exact physiological meaning of the rate constants assigned to the compartments will depend on the modeling assumptions and compartment definitions. For example, a two-tissue compartment model linked by four rate constants is typically sufficient describing a radiotracer that binds to a receptor site in the brain (Fig. 3.2a, b).

Often the number of compartments corresponds to the number of physical spaces within the tissue but may also represent a state. These physiological

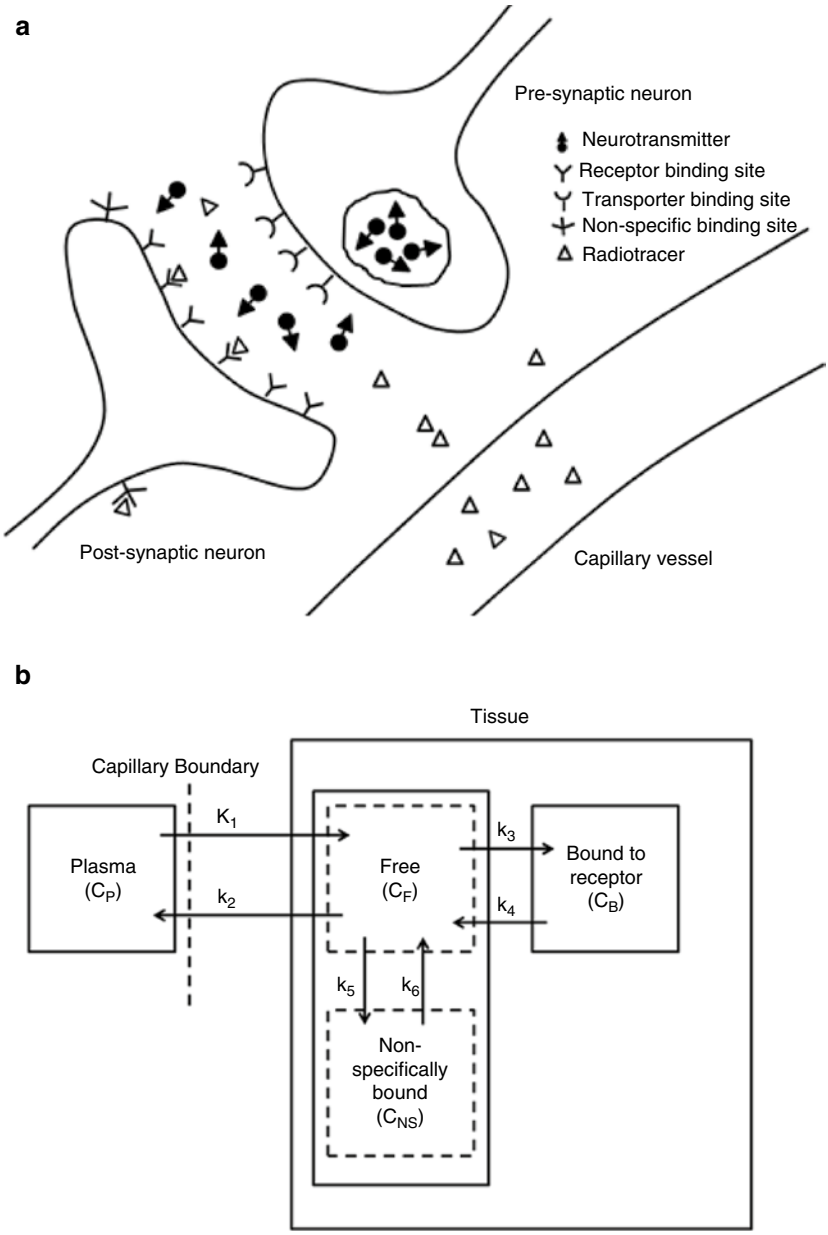

Fig. 3.2 Simplistic representation of the binding of a radiotracer selective for a receptor on the postsynaptic neuron (**b**) A two-tissue compartment model depicting the process in (**a**). The compartments consist of (1) radiotracer in the plasma supplying the tissue, C_P; (2) free radiotracer in the extracellular space, or bound to a nonspecific site, C_{F+NS}; and (3) radiotracer bound to the target receptor, C_B. The rates of exchange between compartments are denoted by the arrows and their associated constants (K_1, k_2, k_3, k_4). The compartment model is considered reversible because the radiotracer is free to leave the bound state and reenter the extracellular space

differences, and others like them, must be considered in the compartment model because they affect how the rate constants are interpreted. The physical scale of the situation depicted in Fig. 3.1 is on the order of 10 μm. A PET scanner, with resolution on the order of mm, cannot distinguish between a radiotracer in the different compartments; thus, the measured PET signal at any given time is the total of the radioactivity in all compartments. The contribution of modeling is to infer how the radiotracer is being transported between the compartments by using mathematical modeling as a basis for understanding the dynamic data measured by the scanner.

The constants describing the rates of exchange between compartments are obtained by solving a coupled series of differential equations (Eqs. 3.1 and 3.2). The measured PET signal is the weighted sum of the blood (C_P), extracellular (C_{F+NS}), and bound compartments (C_B) (Eq. 3.3). The weighting factors (V_P, V_F, V_B) are the fraction of an image pixel that each of the compartments occupies. There are more constants than available equations; therefore, the problem is mathematically underdetermined, and there is not be a single unique set of rate constants that describe the measured data. In the model's application, the rate constants are determined simultaneously using iterative methods, and the solution is restricted to physiologically relevant values. Equations for the model depicted in Fig. 3.1 are:

$$\frac{dC_F}{dt} = K_1 C_P - k_2 C_{F+NS} - k_3 C_{F+NS} + k_4 C_B \tag{3.1}$$

$$\frac{dC_B}{dt} = k_3 C_{F+NS} - k_4 C_B \tag{3.2}$$

$$PET = V_P C_P + V_F C_{F+NS} + V_B C_B \tag{3.3}$$

If the radiotracer freely exchanges between compartments for a sufficient length of time, and the radioactivity concentration in the plasma is held constant, the concentrations in the extracellular and intracellular spaces eventually reach equilibrium. At this point the individual compartment concentrations do not change, and the left side of Eqs. 3.1 and 3.2 are zero. At equilibrium, it is very difficult to accurately separate the individual influx and efflux rate constants for each compartment because of the underdetermined nature of the problem. However, the ratio of rate constants is considered unique and useful for representing the ratio of concentrations of radiotracer in two compartments. The equilibrium ratio is termed a volume of distribution and can be calculated as an appropriate combination of rate constants. By convention, the total volume of distribution, V_T, is the ratio of the radioactivity concentrations in the tissue to that in plasma. For the two-tissue compartment model in Fig. 3.2, V_T is the summation of the distribution volumes in the free compartment and cellular compartments (since V_F and V_B are equal in this case). The distribution volume in the free compartment is also referred to as the non-displaceable distribution volume,

$V_{ND} = C_F/C_P$. The relationship to the rate constants can be derived from Eqs. 3.1 and 3.2 and the equilibrium condition as:

$$V_T = \frac{C_{F+NS}}{C_P} + \frac{C_B}{C_P} = \frac{K_1}{k_2} + \frac{K_1 k_3}{k_2 k_4} = \frac{K_1}{k_2}\left(1 + \frac{k_3}{k_4}\right) \approx \frac{C_T}{C_P} \tag{3.4}$$

where the last approximate equality arises from Eq. 3.4, assuming V_P is small and $V_F = V_B$. The analysis techniques below can be used to quantitatively determine combinations of rate constants even if the system under investigation is not in equilibrium. In this case, a quantitative value can be derived from the dynamic PET data that is directly related to the physiology being studied.

In the brain, the compartment model for receptor imaging has two-tissue compartments. The first corresponds to the radiotracer residing in extracellular space and the second corresponds to the radiotracer bound to the receptor target. The latter tissue compartment is not defined in space but a change in state of the radiotracer from "free" to "bound." The rate constants describing the movement of the radiotracer in the receptor model are as follows: K_1 [mL/g/min] and k_2 [1/min] represent the unidirectional fractional rate constants, corresponding to the influx and efflux of radioligand diffusion across the blood brain barrier, respectively. k_2 is the rate that tracer leaves the extracellular compartment for the plasma, $k_3 = k_{on}B_{avail}$ since this is a tracer experiment, and $k_4 = k_{off}$, the off rate from the transporter [2]. The kinetic parameter of interest is the number of available receptors for binding (B_{avail}) in a brain region compared to that in the free space,

$$\frac{\left(V_T - V_{ND}\right)}{V_{ND}} = \frac{C_B}{C_{F+NS}} = \frac{k_3}{k_4} = \frac{k_{on}B_{avail}}{k_{off}} = \frac{B_{avail}}{K_D} \tag{3.5}$$

where K_D is the disassociation constant. This term is commonly referred to as binding potential (BP).

For a radiotracer that is trapped in a cellular process, whether by incorporation into another molecule, the model has at least one compartment that is irreversible (Fig. 3.3). In this case, the concept of equilibrium distribution volume is not useful. Instead, the rate at which the radiotracer is incorporated into protein is more relevant and related to the rate that the radiotracer enters the irreversible compartment. The flux into the extracellular space is the product of the blood flow and extraction fraction (the probability that a radiotracer molecule will cross the capillary membrane during a single pass through the capillary). The flow and extraction fraction product is the unidirectional rate constant K_1 in the compartment model. Multiplying this quantity by the radiotracer arterial plasma concentration gives an estimate of the rate of transfer of radiotracer into tissue. Let K_1 represent the rate of glucose delivery to the free space. Then the net rate of glucose delivery across the cell membrane can be determined by multiplying K_1 by the fraction of

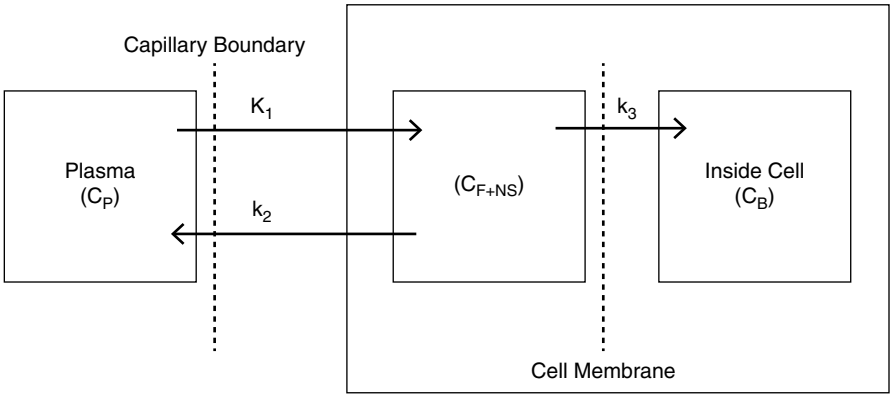

Fig. 3.3 A two-tissue compartment model representing the trapping of a radiotracer in a cell

radiotracer that leaves the free space and enters the cell. This quantity represents the net influx of a radiotracer into the cell.

$$K_{\text{influx}} = K_1 \frac{k_3}{k_2 + k_3} \tag{3.6}$$

This is represented in Fig. 3.3.

3.3.3.2 Input Function

The concentration of the radiotracers in tissue depends on the time varying concentration of the radiotracers in arterial blood. The input function can be determined by measuring arterial blood samples. Following a bolus injection, blood samples are initially drawn at a high frequency and as the dose distributes throughout the body, blood samples are collected less frequently. The blood is then centrifuged to separate blood cells and proteins from the plasma. Only radioactivity contained in the plasma fraction is measured because it represents the amount of radiotracer that is free to cross the capillary boundary and enter the tissue.

Another technique to derive a suitable input function is to measure it directly from image data. This technique entails placement of a large ROI over an arterial structure, such as the left ventricle, aorta, or another large artery. If number and proportion of labeled metabolites in blood are known or they are rapidly and efficiently excreted from the bloodstream, this approach may permit comparisons between kinetic parameter estimates and actual arterial samples [3, 4].

A third technique to estimate an input function is the reference region approach which is widely used in receptor imaging [5]. A reference region is defined as a tissue region that is identical in all aspects to the region of interest except there are negligible specific binding sites. This technique provides several advantages

compared to arterial sampling including reduction in discomfort to the patient, need for fewer personnel, and reduced errors in the compartment model parameter estimates because the reference region and region of interest are derived from the same image data. The reference procedure introduces a second compartment model that describes the delivery of radioligand to the interstitial space of the reference region. This in turn permits construction of a mathematical model that describes the plasma input in terms of the reference region and the estimation of kinetic parameters.

3.3.3.3 Modeling Assumptions

There are a number of implicit assumptions made when using compartment models to describe the kinetics of a radiotracer in a complex biological system. The first and most important assumption is that the mass of injected radiotracer (labeled and unlabeled) is a trace amount. That is, its concentration is negligible to the extent that is does not alter in any way the process that it is intended to mimic. This is equivalent to saying that so little compound is administered that it does not produce even the slightest pharmacological effect. This assumption is met when the specific activity, which is radioactivity divided by the total mass (GBq/micromole), of the tracer is sufficiently high. Second, the endogenous molecule mimicked by the radiotracer must be at steady state throughout the duration of the experiment. This condition is met if there are no changes in external factors such as administration of compounds that alter the physiological state or compete with the radiotracer for binding in the tissue. Thirdly, the mixing of the radiotracer with other molecules in the compartment must occur at a substantially faster rate than its exchange between compartments. Often this assumption is referred to as instantaneous mixing. Lastly, the labeled isotope does not change the behavior of the radiotracer in relation to the stable label. For example, [C-11]raclopride is expected to behave exactly as raclopride containing stable carbon. This is termed the isotope effect.

3.3.4 Graphical Transformation

A common approach to estimating kinetic parameters that is often performed in parallel with compartmental modeling is graphical analyses because it is simple and does not require complete knowledge of the underlying physiology of the system. Current graphical methods only require knowledge that the radiotracer is either freely reversible in all compartments or irreversibly trapped by at least one compartment, regardless of the number. In both cases, transformations are performed on the time and measured radioactivity so that, when plotted, the graph approaches a straight line at later time points.

The Patlak plot is a graphical method that has been used in analyzing [F-18] FDG data because it assumes at least one compartment is irreversibly trapped [6, 7]. This compartment would represent the phosphorylation of [F-18]FDG. This

graphical approach estimates fractional uptake rate of [F-18]FDG described in the two-tissue compartment model (Fig. 3.3). The approach works, because after the reversible compartments reach quasi-equilibrium, the change in radioactivity levels in tissue is due solely to trapping in the irreversible compartment. The data transformation described by Patlak is such that when equilibrium in the reversible and plasma compartments is achieved, the plot approaches a straight line and the slope of the line is the influx constant, K_{influx}. A second graphical approach is applicable when all compartments are reversible and is referred to as Logan analysis [8, 9]. Such an analysis may be appropriate for tracers that are reversible, such as receptor binding studies. Following the graphical transformation, the slope of the linear region is the distribution volume. Both the Patlak and Logan graphical transformation methods can be used with a reference tissue input if arterial blood is not measured.

3.4 Application of PET in Pharmacology

The PET tracer technique permits the characterization of in vivo drug interactions with specific protein targets while not perturbing the physiological system. Choosing an appropriate radiotracer, of high affinity for a target of interest, can provide insights into neurochemical interactions related to behavioral observations. Some of these insights include drug interactions with neurotransmitter receptors and transporters, changes in cerebral blood flow, and alterations of cerebral metabolism. A straightforward application of PET is characterization of the radiotracer uptake kinetics and biodistribution, including overall magnitude (SUV), time-to-peak uptake, and the washout phase. This simplistic analysis has lead to several notable contributions including radiolabeling of cocaine and methylphenidate with carbon-11 to examine their in vivo kinetics in humans [10, 11]. These psychostimulants have roughly equal affinity for all three monoamine transporter systems (dopamine, serotonin, and norepinephrine); however, their kinetics vary considerably. The washout phase of methylphenidate is substantially slower than cocaine, and this observation is thought to contribute to differences in abuse potential between these agents despite their similar binding profiles. Radiolabeling of drugs has led to a number of insights into how behavioral outcomes relate to drug kinetic profiles and their interactions and continues to be a powerful technique with PET [12, 13].

Compartment modeling analysis can lead to a deeper understanding of underlying physiological processes in vivo by estimating rate constants that govern radiotracer uptake. One aspect is calculation of binding potential, which is related to the total number of available binding sites and plays an essential role examining the acute and chronic integrity of protein targets [2]. Furthermore, binding potential may be calculated in the presence of competitive drug binding to determine occupancy at the target site [14]. Occupancy experiments are generally conducted in two steps, an initial study in the presence of no drugs to measure the baseline density followed by exposure to the drug then immediately repeating the study to measure

the density with drug on board. The ratio of the measured binding potential between these two states can be used to calculate the occupancy of drug in the target tissue,

$$\text{Occupancy } \% = 100 \times \left(1 - \frac{\text{BP}_{\text{drug on-board}}}{\text{BP}_{\text{baseline}}} \right)$$

Calculation of occupancy has been crucial in determining the relationship between drug concentration in vivo and pharmacological onset. For many psychostimulants, it has been determined using PET that a minimum drug occupancy of at least 65 to 75 % is needed to observe behavioral changes [11, 15, 16]. These experiments can be conducted in a single session starting with an initial baseline phase followed by a drug chase that displaces the baseline signal [17, 18].

Similar to the occupancy protocol, PET has been used to measure drug-induced endogenous neurotransmitter release. In this case, the drug administered evokes release of endogenous neurotransmitters that compete with the radiotracer for binding. The classic case is displacement of [C-11]raclopride from D2/D3 receptors by release of dopamine after administration of amphetamine or similar analogues. This experiment is different than drug occupancy described above because the displacement action is due to competitive interactions with an endogenous molecule rather than an exogenously administered drug. Again, the binding potential can be calculated using compartmental modeling concepts and the difference between the baseline and drug induction are typically compared.

Lastly, assessments in changes of cerebral metabolism are useful for monitoring changes in brain activity under various drug actions. The actual calculation of regional cerebral glucose metabolism is complicated by the need for arterial blood sampling to determine the input function. Secondly, FDG imaging does not follow the complete glucose metabolic pathway, and a conversion factor is needed to relate FDG metabolism to glucose metabolism, called the lumped constant. FDG data are compared using SUV quantitation or by group analysis packages such as statistical parametric mapping [19]. Hyper- and hypometabolic changes can be determined in these studies compared to a baseline or normal control population [20]. These techniques have been used extensively in studies of acute and chronic drug interactions [16, 20–23].

PET offers a great value in translational sciences from simple experiments to measure brain penetrability of radiolabeled drugs and their biodistribution to more sophisticated studies including calculation of occupancy using radiotracer displacement protocols.

3.5 Challenges to Using PET

The uptake and distribution of radiolabled molecules will depend, in part, on the laboratory conditions during the study including the environment, normal physiology, and use of anesthetics. These factors add variability to the outcome

measurement and anticipating such pitfalls can improve the quality of the data. Below is a brief discussion of some particular challenges.

PET imaging requires that the subject be still throughout the exam. Motion on the order of the resolution of the scanner (by as little as a few millimeters) degrades the achievable reconstructed resolution, reduces contrast, and may lead to the erroneous application of attenuation correction. In dynamic PET imaging, scan durations may be in excess of 1 h, and invariably a subject will shift a small amount to ease discomfort over this duration. A motion event may be voluntary or involuntary. For example, motion such as moving an arm to tend to an itch or respiratory motion during normal breathing. Additional movement may result from the subject's physiological state such as muscle tremors or forgetting instructions. It is desirable to correct for motion events as best as possible by either closely monitoring the subject or using software tools. In brain imaging there are generally two types of motion to consider: (1) motion between the emission (PET) and attenuation scans and (2) motion within an emission frame. The former is relatively easy to address using software to align the transmission data with the emission data and re-reconstruct the PET images. The latter presents more challenges and has been addressed by subdividing the emission data into shorter frame durations, throwing out the time duration that included the motion or incorporating more sophisticated motion correction algorithms in the reconstruction. Head restraints help prevent a great deal of these troubles but not all.

With the exception of a few laboratories, anesthesia is used in the preclinical imaging environment to sedate animals and maintain the quiescent state needed for PET imaging. There is ample evidence showing that anesthesia alters the physiological state of an animal including blood flow, metabolism, and neurotransmitter expression in the brain [24–26]. A large number of commonly used anesthetics including ketamine and isoflurane have been shown to alter brain homeostasis. Many of the effects listed above are dose and species dependent. Minimizing physiological alterations secondary to anesthetics generally entails careful monitoring and simplifying laboratory procedures so they can be easily replicated.

A well-controlled environment including warming devices and monitoring equipment is crucial to a successful study. Control of these conditions is most important in animal imaging, where the mouse, rat, or nonhuman primate is sedated during the study. A reduction in an animal's core body temperature results in constriction of blood vessels and redistribution of blood to conserve vital functions. These changes will alter the uptake of radiotracers, generally reducing the contrast.

3.6 Dosimetry

Radiation dosimetry refers to the amount of energy deposited in an organ and the whole body (i.e., dose) resulting from the internal administration of radionuclides. This information is important in assessing deterministic (e.g., cataract,

radiotoxicity) and stochastic (cancer induction) effects from radiation exposure. Some regulatory bodies limit the amount of internally deposited radiation dose; therefore, estimating internal dose from radiopharmaceutical injections may be warranted. The purpose of this section is to provide an overview of how absorbed dose is estimated for internally deposited radiolabeled molecules.

The absorbed dose is a function of the radiotracer's kinetics, the number and energy of the emitted radiations, and the organ sizes and positions. The latter can be obtained from anatomical imaging (either CT or MR); however, capturing the radiotracer kinetics for calculation of individual absorbed doses requires long scan times and is not feasible in a clinical setting. Thus, methodology has been developed to estimate dose based on anthropomorphic phantoms that is then extrapolated to populations of subjects. The following sections briefly describe the Medical Internal Radiation Dose Committee (MIRD) method and present published absorbed dose results for some common radiotracers used in PET research.

3.6.1 Acquisition Protocols and Calculation of Time Activity Curves

Serial whole-body scans spanning from the head to mid-thigh are used to gather the radiotracer kinetics for absorbed dose calculations. Bed durations are typically short following administration of the radioactivity to measure the blood pool changes and then gradually increase to capture longer retention kinetics within organs. Fast excretion kinetics may necessitate that scans begin at the mid-thigh rather than the head in order to capture the initial elimination of the tracer and its metabolites by the kidney before it is taken up into tissue. As with compartment modeling, the total scan duration that a subject can tolerate is limited to about 2 h. Information beyond this point is estimated by extrapolation assuming only physical decay beyond the last measured data point or by using more sophisticated methods of curve fitting and compartment modeling.

3.6.2 Absorbed Dose

To standardize the dose calculation, Stabin et al., 1996, published the MIRDOSE software which calculates the internally deposited dose from the number of decays that take place in each organ [27]. The software includes the International Commission on Radiological Protection (ICRP) GI tract model and Cloutier dynamic bladder model (ICRP 30) which account for radioactivity moving through these excretory systems [28, 29]. The software provides the absorbed dose and effective dose per unit of administered radioactivity as detailed in the MIRD primer [30]. The MIRDOSE code has since been updated to comply with FDA 510k rules and renamed OLINDA/EXM [31]. OLINDA contains all the features of MIRDOSE

with some additions such as an expansion of the radionuclide library, the ability to change organ masses to better match patient populations, and updates to absorbed fractions of marrow, bone, and skin.

The organ dose result from the MIRD schema is reported in units of equivalent dose as defined by the ICRP that are then normalized by the administered radioactivity [mSv/mBq]. The equivalent dose (Sv) is the absorbed dose (Gy) multiplied by a weighting factor called the relative biological effectiveness (RBE). The RBE is proportional to the amount of energy needed to produce a biological effect relative to a standard (200 keV x-rays). It is an empirical weighting factor that ranges from 1, for x-rays, to 20, for alpha particles. For establishing annual limits, the ICRP introduced the effective dose to take into account the probability of stochastic effects such as cancer caused by radiation-induced cell mutations. The effective dose is a sum of the individual organ contributions to the whole-body stochastic radiation burden, for which each organ is multiplied by a weighting factor proportional to an organ's susceptibility to cancer induction [32]. This effective dose is used in comparisons of radiation risk and for recording cumulated radiation burden. It is also of interest to know which organ receives the highest equivalent dose. This organ is referred to as the critical organ. Often the limit for an individual organ dose is reached before the limit established for the whole body. The US Food and Drug Administration in Title 21 CFR Part 361 suggests limits for whole-body radiation dose to adult research subjects to less than 30 mSv for a single injection and 50mSv annually. A single organ cannot receive more than 50 mSv in a single injection and 150 mSv annually. These constraints on dose will limit the maximum number of injections for research subjects.

The whole-body effective dose per unit administered radioactivity for a variety of Fluorine-18 labeled compounds typically ranges between 0.015 and 0.025 mSv/MBq (6–10 mSv for 370 MBq). The whole-body dose is a function of isotope half-life, but the reduction in dose from using short-lived isotopes is often offset by the need to inject more activity to provide suitable counting statistics in the image. The dose per administered activity is roughly greater by a factor of 3 for the ^{18}F-labeled compounds.

3.7 Conclusions

The application of compartmental modeling in PET provides a simplified mathematical interpretation of the time varying uptake of radiotracers that is used to extract physiological information. Prior to application of a model, it is important to understand both the biochemical behavior of the injected radiotracer and underlying physiology of the disease. This information is crucial for choosing an appropriate number of compartments and rate constants and in the interpretation of the estimated parameters. A well-constructed model will give more insight into the physiological mechanisms that characterize a disease and be more sensitive to changes in the disease state.

References

1. Reivich M, Kuhl D, Wolf A et al (1979) The [18F]fluorodeoxyglucose method for the measurement of local cerebral glucose utilization in man. Circ Res 44:127–137
2. Mintun MA, Raichle ME, Kilbourn MR et al (1984) A quantitative model for the in vivo assessment of drug binding sites with positron emission tomography. Ann Neurol 15: 217–227
3. Raylman RR, Caraher JM, Hutchins GD (1993) Sampling requirements for dynamic cardiac PET studies using image-derived input functions. J Nucl Med 34:440–447
4. Hoekstra CJ, Hoekstra OS, Lammertsma AA (1999) On the use of image-derived input functions in oncological fluorine-18 fluorodeoxyglucose positron emission tomography studies. Eur J Nucl Med 26:1489–1492
5. Lammertsma AA, Hume SP (1996) Simplified reference tissue model for PET receptor studies. Neuroimage 4:153–158
6. Patlak CS, Blasberg RG, Fenstermacher JD (1983) Graphical evaluation of blood-to-brain transfer constants from multiple-time uptake data. J Cereb Blood Flow Metab 3:1–7
7. Patlak CS, Blasberg RG (1985) Graphical evaluation of blood-to-brain transfer constants from multiple-time uptake data. Generalizations. J Cereb Blood Flow Metab 5:584–590
8. Logan J, Fowler JS, Volkow ND et al (1996) Distribution volume ratios without blood sampling from graphical analysis of PET data. J Cereb Blood Flow Metab 16:834–840
9. Logan J, Fowler JS, Volkow ND et al (1990) Graphical analysis of reversible radioligand binding from time-activity measurements applied to [N-11C-methyl]-(−)-cocaine PET studies in human subjects. J Cereb Blood Flow Metab 10:740–747
10. Volkow ND, Wang GJ, Fischman MW et al (1997) Relationship between subjective effects of cocaine and dopamine transporter occupancy. Nature 386:827–830
11. Volkow ND, Wang GJ, Fowler JS et al (1996) Relationship between psychostimulant-induced "high" and dopamine transporter occupancy. Proc Natl Acad Sci U S A 93:10388–10392
12. Kimmel HL, Negus SS, Wilcox KM et al (2008) Relationship between rate of drug uptake in brain and behavioral pharmacology of monoamine transporter inhibitors in rhesus monkeys. Pharmacol Biochem Behav 90:453–462
13. Volkow ND, Ding YS, Fowler JS et al (1996) Cocaine addiction: hypothesis derived from imaging studies with PET. J Addict Dis 15:55–71
14. Laruelle M, Slifstein M, Huang Y (2002) Positron emission tomography: imaging and quantification of neurotransporter availability. Methods 27:287–299
15. Howell LL, Murnane KS (2008) Nonhuman primate neuroimaging and the neurobiology of psychostimulant addiction. Ann N Y Acad Sci 1141:176–194
16. Howell LL, Murnane KS (2011) Nonhuman primate positron emission tomography neuroimaging in drug abuse research. J Pharmacol Exp Ther 337:324–334
17. Votaw JR, Howell LL, Martarello L et al (2002) Measurement of dopamine transporter occupancy for multiple injections of cocaine using a single injection of [F-18]FECNT. Synapse 44:203–210
18. Endres CJ, Kolachana BS, Saunders RC et al (1997) Kinetic Modeling of [11C]Raclopride: combined PET-Microdialysis studies. J Cereb Blood Flow Metab 17:932–942
19. Friston KJ, Frith CD, Liddle PF et al (1991) Comparing functional (PET) images: the assessment of significant change. J Cereb Blood Flow Metab 11:690–699
20. Henry PK, Murnane KS, Votaw JR et al (2010) Acute brain metabolic effects of cocaine in rhesus monkeys with a history of cocaine use. Brain Imaging Behav 4:212–219
21. Volkow ND, Fowler JS, Wang GJ et al (2004) Dopamine in drug abuse and addiction: results from imaging studies and treatment implications. Mol Psychiatry 9:557–569
22. Volkow ND, Fowler JS, Wolf AP et al (1991) Changes in brain glucose metabolism in cocaine dependence and withdrawal. Am J Psychiatry 148:621–626
23. Volkow ND, Wang GJ, Ma Y et al (2005) Activation of orbital and medial prefrontal cortex by methylphenidate in cocaine-addicted subjects but not in controls: relevance to addiction. J Neurosci 25:3932–3939

24. Kaisti KK, Metsähonkala L, Teräs M et al (2002) Effects of surgical levels of propofol and sevoflurane anesthesia on cerebral blood flow in healthy subjects studied with positron emission tomography. Anesthesiology 96:1358–1370
25. Matsumura A, Mizokawa S, Tanaka M et al (2003) Assessment of microPET performance in analyzing the rat brain under different types of anesthesia: comparison between quantitative data obtained with microPET and ex vivo autoradiography. Neuroimage 20:2040–2050
26. Alstrup AK, Smith DF (2013) Anaesthesia for positron emission tomography scanning of animal brains. Lab Anim 47:12–18
27. Stabin MG (1996) MIRDOSE: personal computer software for internal dose assessment in nuclear medicine. J Nucl Med 37:538–546
28. ICRP (1988) Radiation dose to patients from radiopharmaceuticals. Publication 53. 18/1–4
29. Cloutier RJ, Watson EE, Rohrer RH et al (1973) Calculating the radiation dose to an organ. J Nucl Med 14:53–55
30. Loevinger R, Berman M (1968) A formalism for calculation of absorbed dose from radionuclides. Phys Med Biol 13:205–217
31. Stabin MG, Sparks RB, Crowe E (2005) OLINDA/EXM: the second-generation personal computer software for internal dose assessment in nuclear medicine. J Nucl Med 46:1023–1027
32. Harrison JD, Streffer C (2007) The ICRP protection quantities, equivalent and effective dose: their basis and application. Radiat Prot Dosimetry 127:12–18